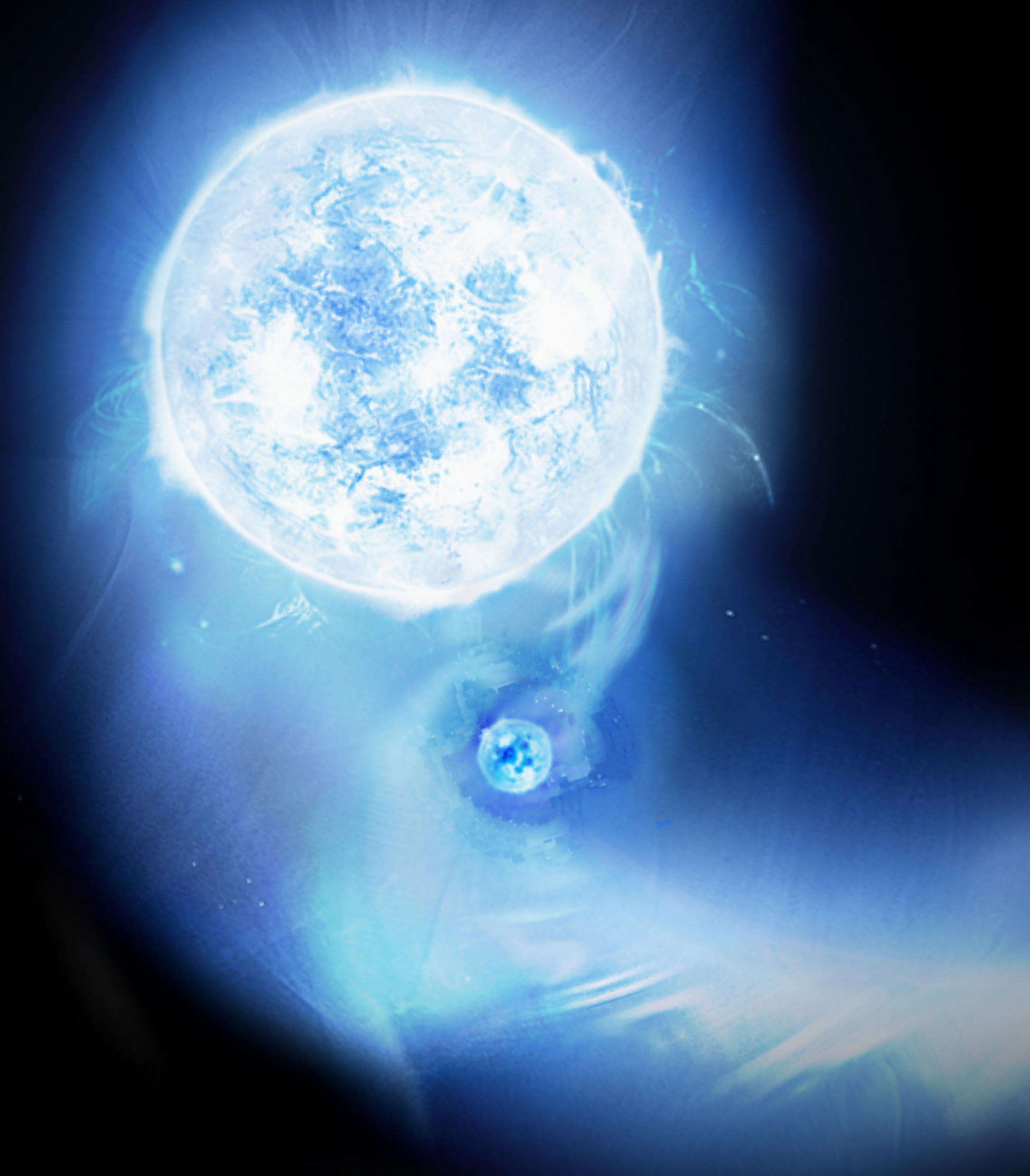

XMM-Newton observations of the peculiar Be X-ray binary A0538-66

MICHELA RIGOSELLI[1]

Caterina Tresoldi[1,2], Lorenzo Ducci[3,4], Sandro Mereghetti[1]

1 INAF, IASF Milano

2 Università degli Studi di Milano

3 Institut fuer Astronomie und Astrophysik Tuebingen

4 ISDC, University of Geneva

06/06/2024 — Madrid

A0538—66

- NS / Be X-ray binary in the LMC (small $N_H=9x10^{20}$ cm^{-2} and known d=50 kpc)
- Super-Eddington accretion and detection of pulsations only in 1980 (P=69 ms, PF~10%)

Skinner+ 1982
Nature

A0538—66

- NS / Be X-ray binary in the LMC (small N_H=9x10^{20} cm^{-2} and known d=50 kpc)
- Super-Eddington accretion and detection of pulsations only in 1980 (P=69 ms, PF~10%)
- Many X-ray observations since 1977, two states:
  - Flaring activity $L_X \sim 10^{36} - 10^{39}$ erg/s lasting from hours to days
  - Quiescent phase $L_X \sim 10^{34} - 10^{36}$ erg/s characterized by constant emission

Skinner+ 1982 Nature

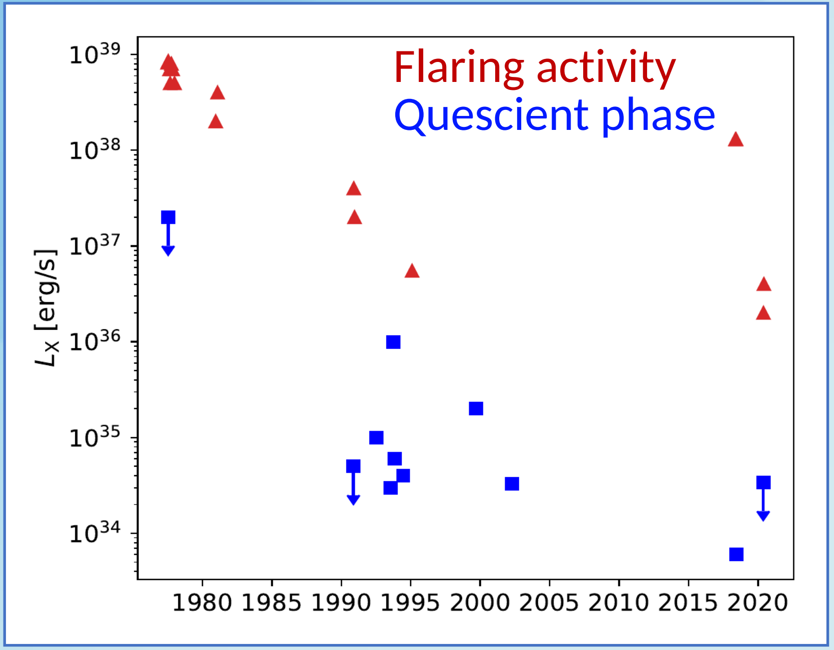

A0538−66

- NS / Be X-ray binary in the LMC (small N_H=9x10^{20} cm^{-2} and known d=50 kpc)
- Super-Eddington accretion and detection of pulsations only in 1980 (P=69 ms, PF~10%)
- Many X-ray observations since 1977, two states:
  - Flaring activity $L_X \sim 10^{36} - 10^{39}$ erg/s lasting from hours to days
  - Quiescent phase $L_X \sim 10^{34} - 10^{36}$ erg/s characterized by constant emission
- Activity does not correlate with the orbital phase

Skinner+ 1982 Nature

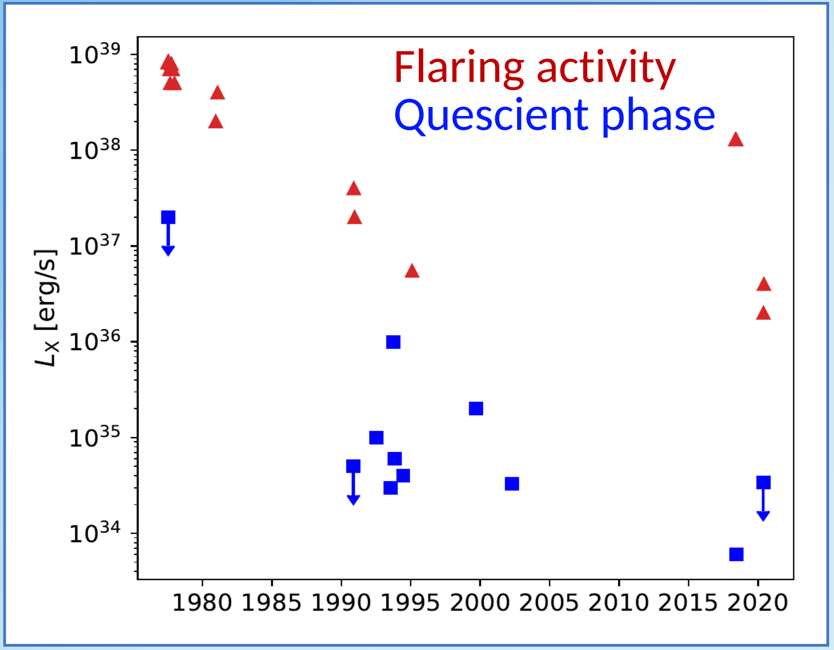

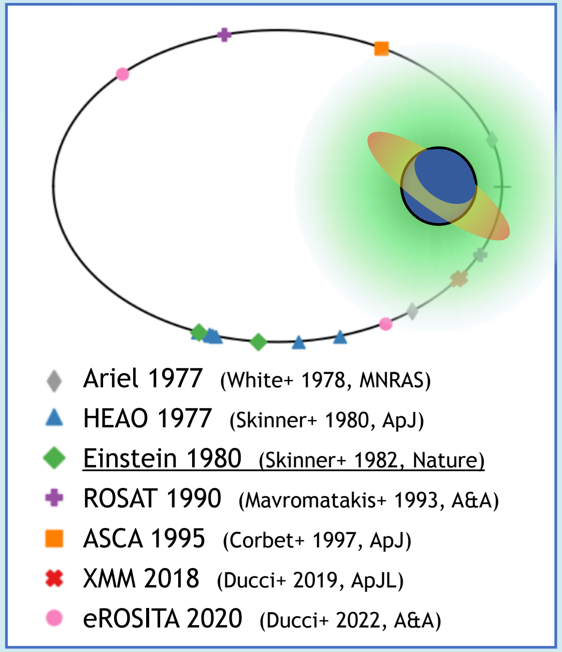

A0538—66

- NS / Be X-ray binary in the LMC (small N_H=9x10^{20} cm^{-2} and known d=50 kpc)
- Super-Eddington accretion and detection of pulsations only in 1980 (P=69 ms, PF~10%)

Skinner+ 1982 Nature

- Many X-ray observations since 1977, two states:
  - Flaring activity $L_X \sim 10^{36} - 10^{39}$ erg/s lasting from hours to days
  - Quiescent phase $L_X \sim 10^{34} - 10^{36}$ erg/s characterized by constant emission
- Activity does not correlate with the orbital phase, but with the presence of the Be disk

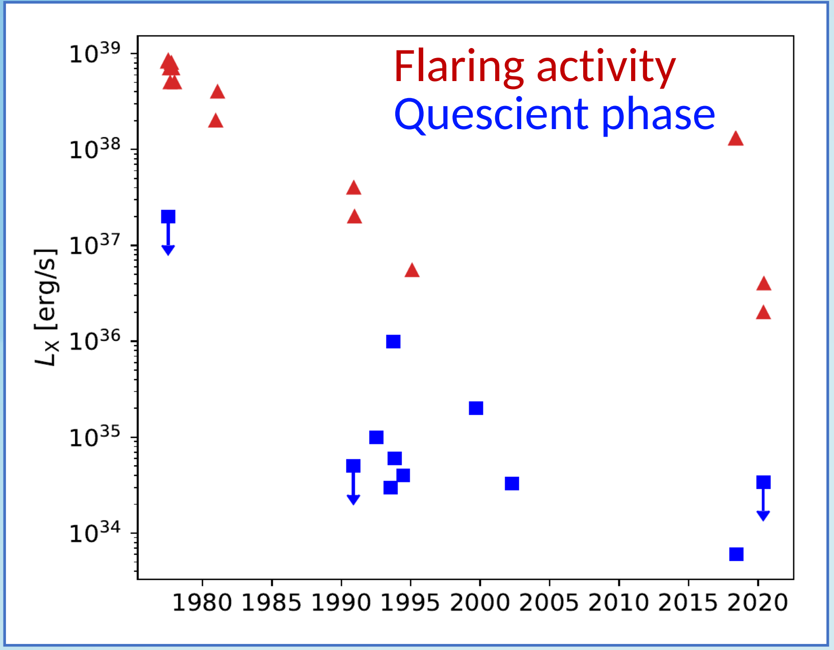

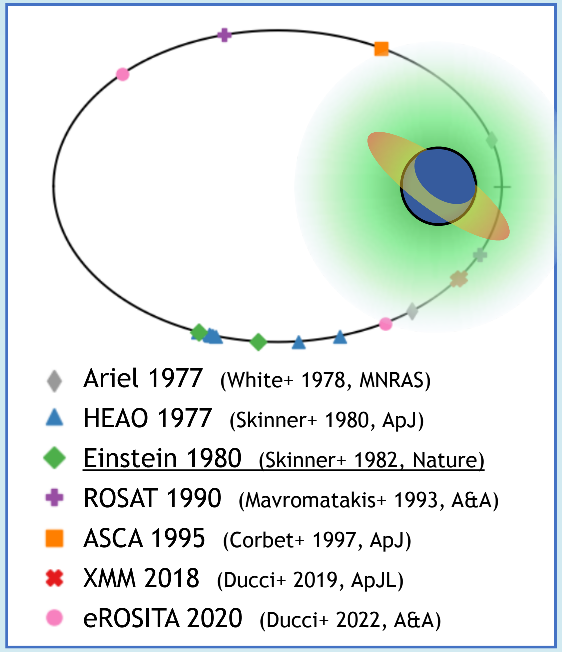

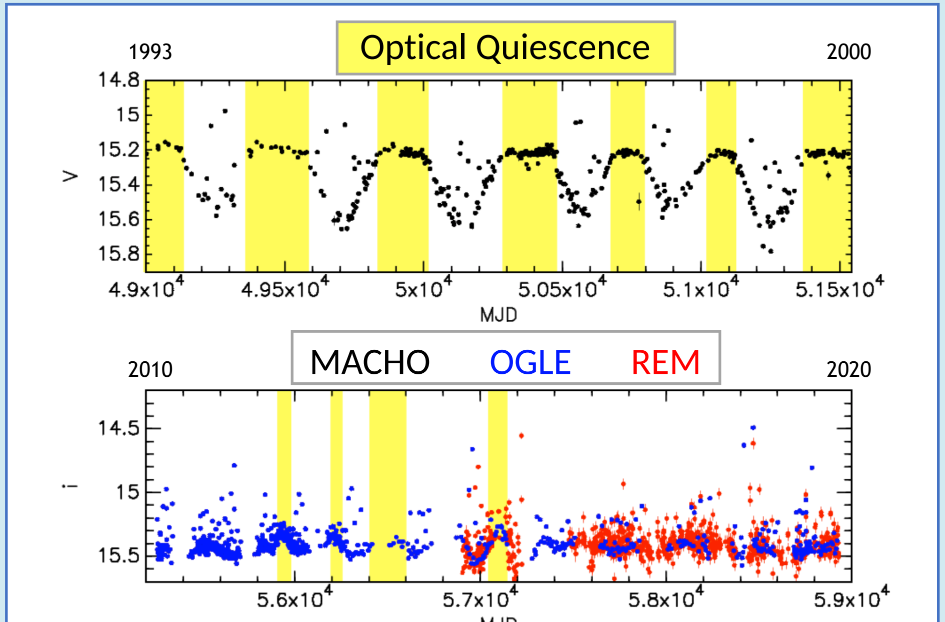

Ducci+ 2022, A&A

A0538—66 with XMM-Newton

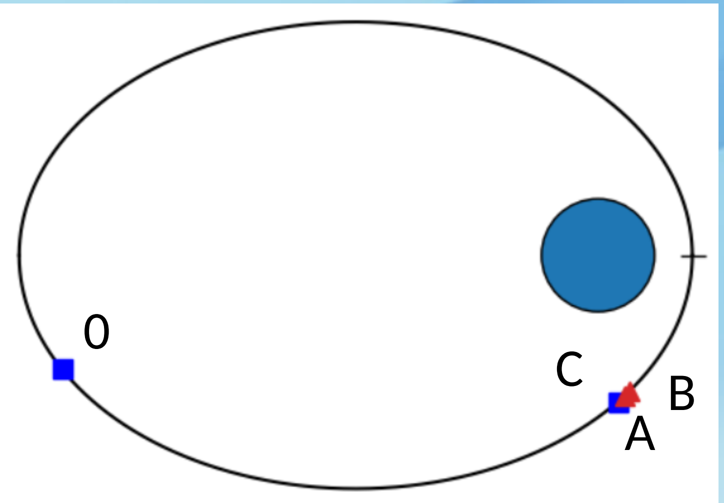

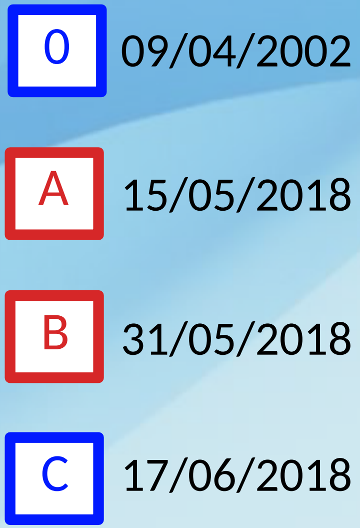

Four XMM-Newton observations:

- One archival obs, far from periastron (0)
- Three obs close to the periastron in three consecutive orbits (A, B and C)

* Ducci et al. 2019 requested and analyzed A, B and C and found peculiar bursting activity in A and B, constant emission in C
* They interpreted the onset of rapid bursts in A and B with spherically simmetric accretion modulated by a magnetic gating mechanism

Kreshmar+ 2004, 5th INTEGRAL Workshop
Ducci+ 2019, ApJL

A0538—66 with XMM-Newton

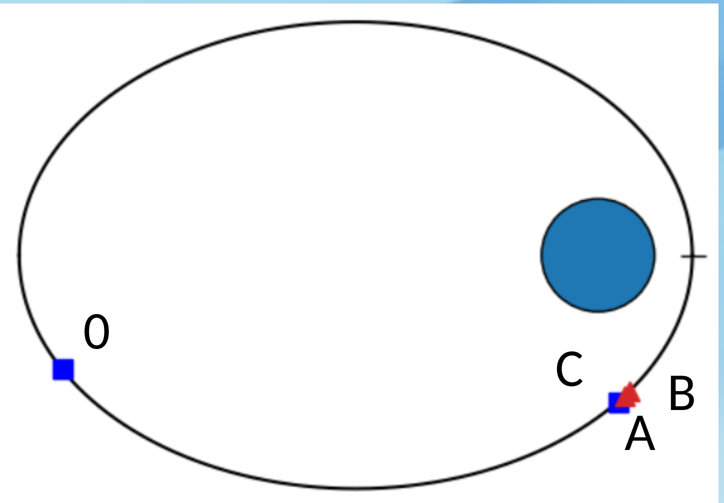

0	09/04/2002
A	15/05/2018
B	31/05/2018
C	17/06/2018

Four XMM-Newton observations:

- One archival obs, far from periastron (0)
- Three obs close to the periastron in three consecutive orbits (A, B and C)

✴ Ducci et al. 2019 requested and analyzed A, B and C and found peculiar bursting activity in A and B, constant emission in C

✴ They interpreted the onset of rapid bursts in A and B with spherically simmetric accretion modulated by a magnetic gating mechanism

Our new analysis:

✴ Timing analysis with Bayesian blocks

✴ Analysis of A/B 'count-rate' resolved spectra and of 0 and C averaged spectra

Kreshmar+ 2004, 5th INTEGRAL Workshop
Ducci+ 2019, ApJL

Timing Analysis

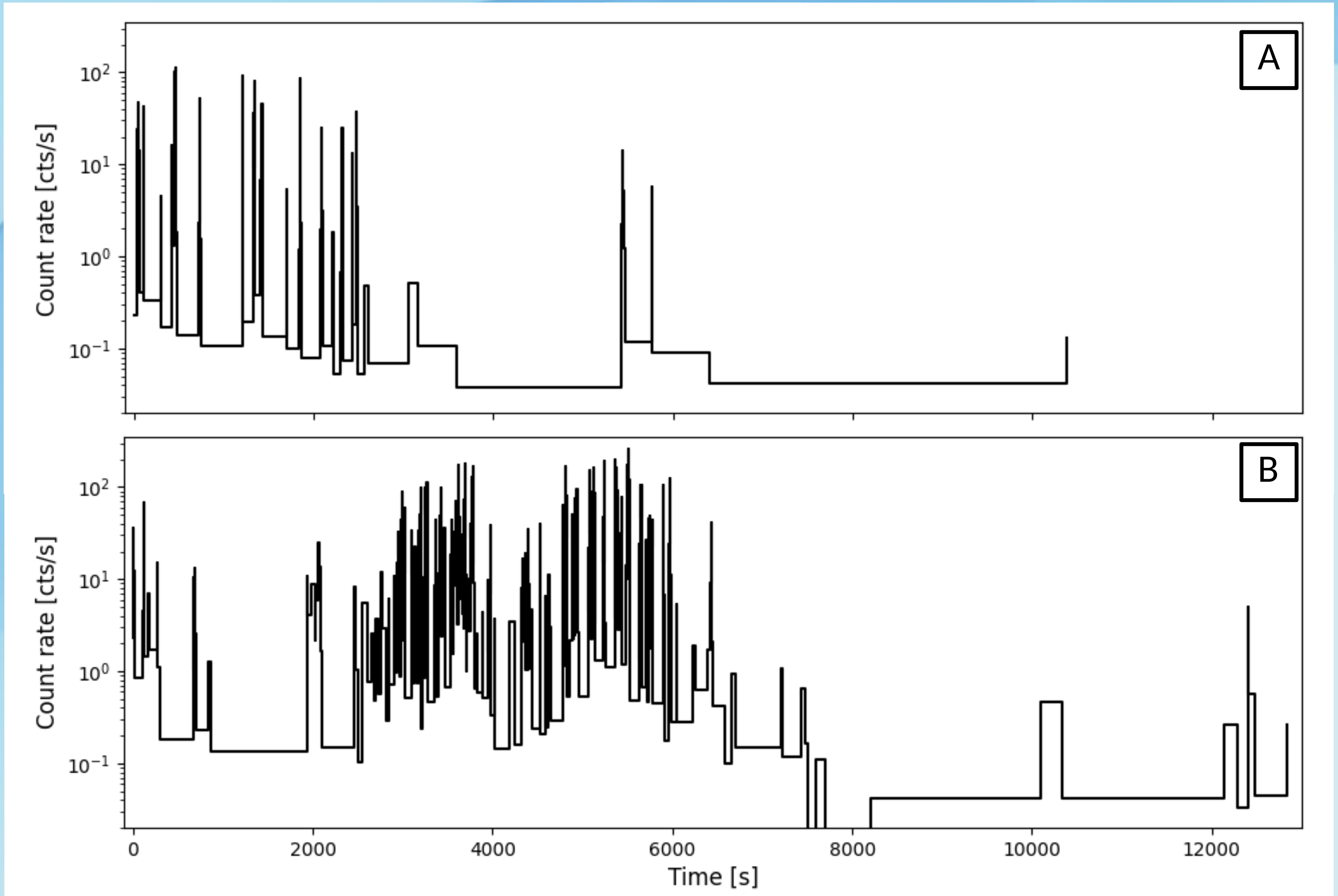

$\Delta t \sim 0.5—50$ s

$\Delta L \sim 100—1000$

MR+ in prep.

Timing Analysis

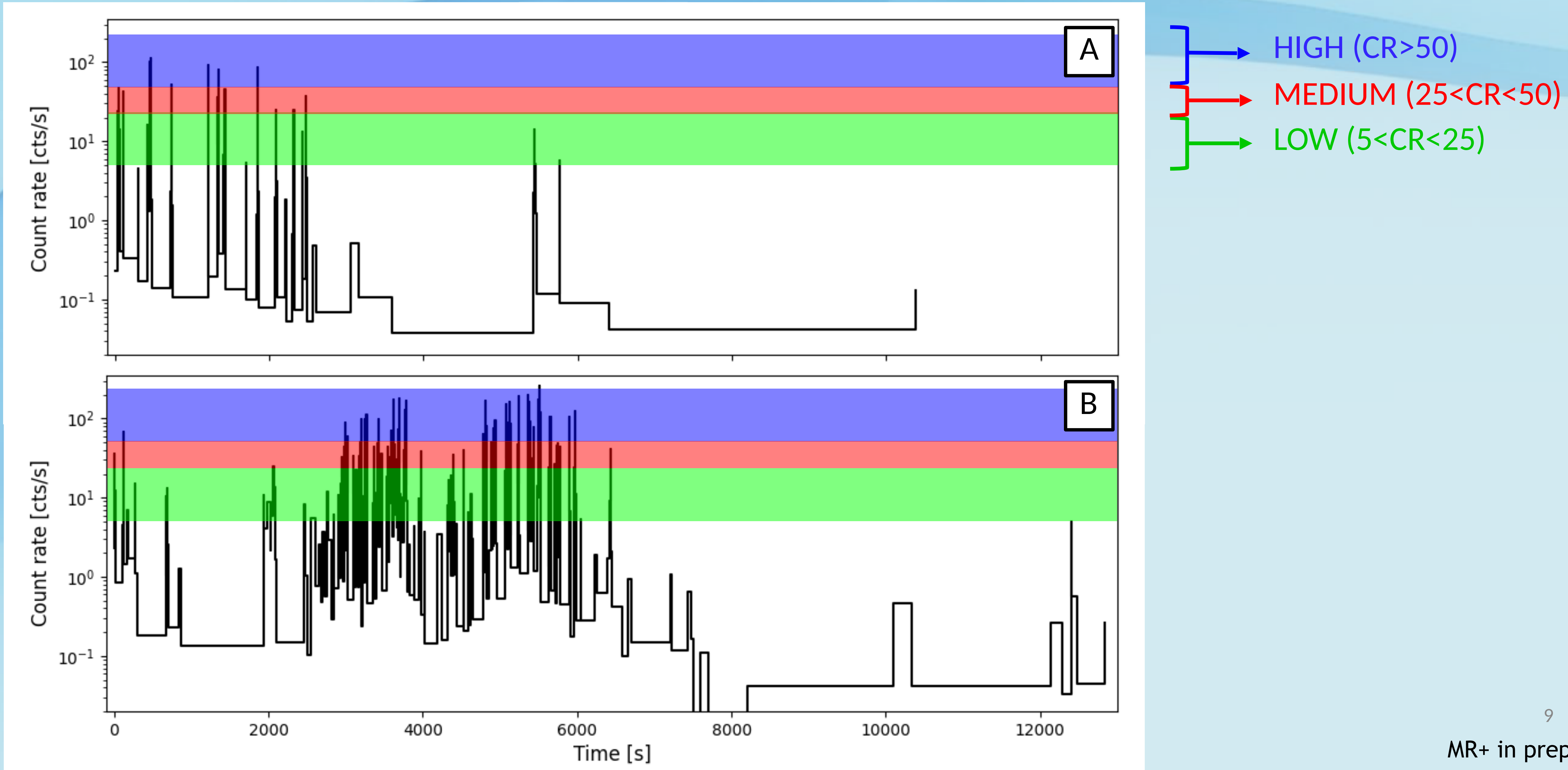

MR+ in prep.

Timing Analysis

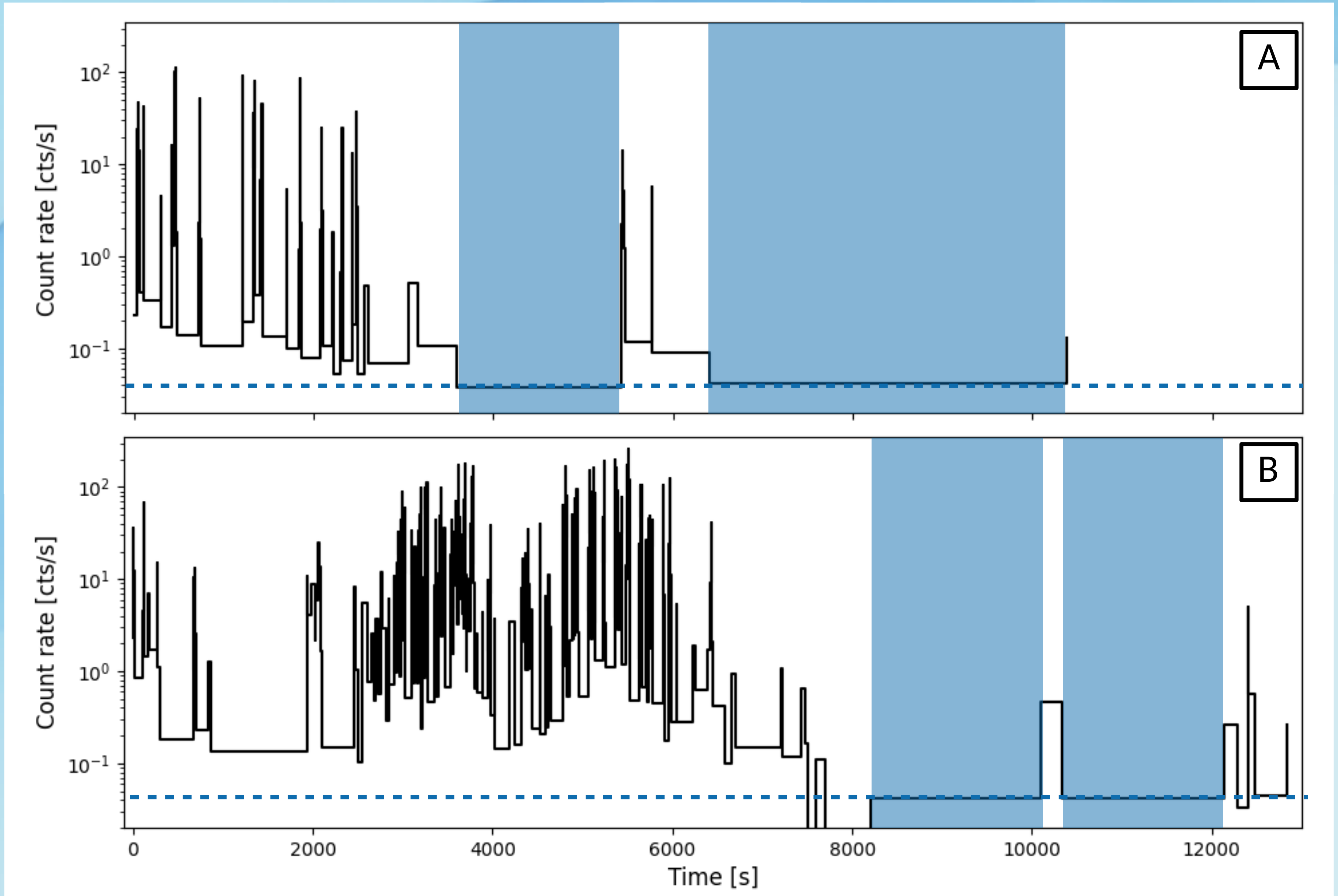

qAB

No bursting activity lasting ~5.5 ks (A), ~3.5 ks (B) and having CR~0.04 cts/s

MR+ in prep.

Spectral Analysis — CR resolved Bursts

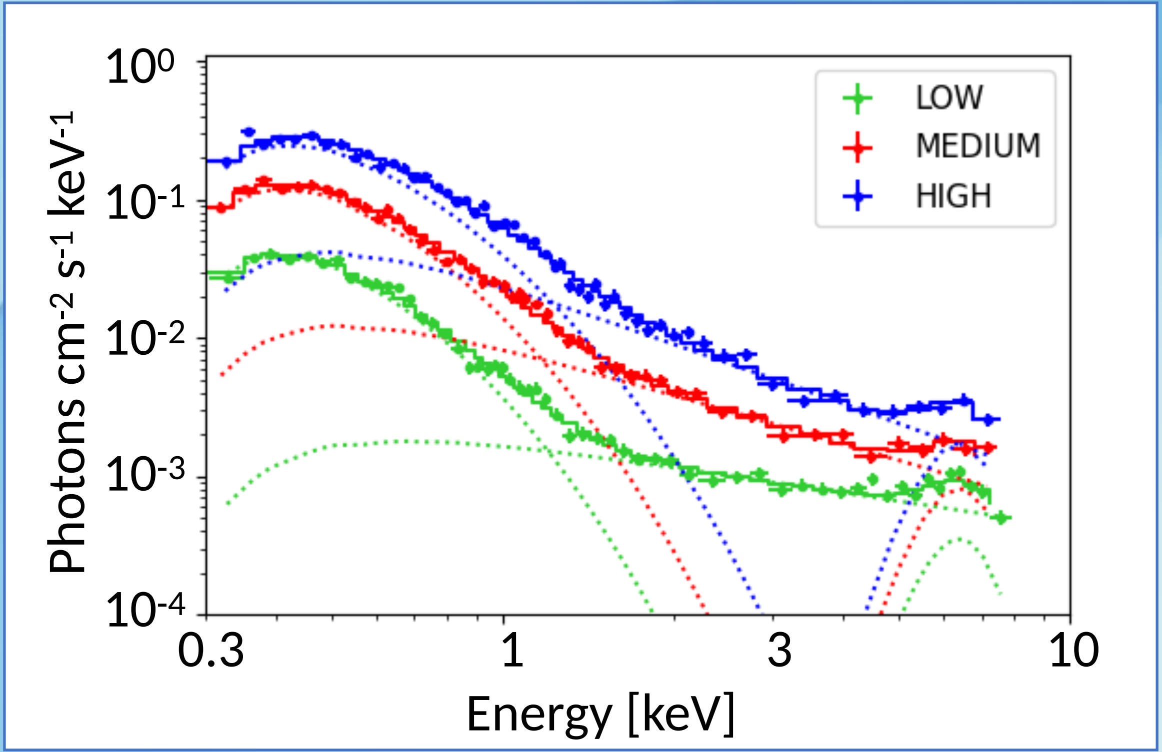

Luminosities 0.3—10 keV:

$1.33 \pm 0.02 \times 10^{38}$ erg/s

$6.13 \pm 0.02 \times 10^{37}$ erg/s

$2.45 \pm 0.05 \times 10^{37}$ erg/s

- Composite Spectrum:
  - soft thermal component (kT~0.2 keV, ~30—40% F_{TOT})
  - hard non-thermal component (Γ~1.5)
  - broad emission line E=6.4 keV, σ~1 keV

MR+ in prep.

Spectral Analysis — CR resolved Bursts

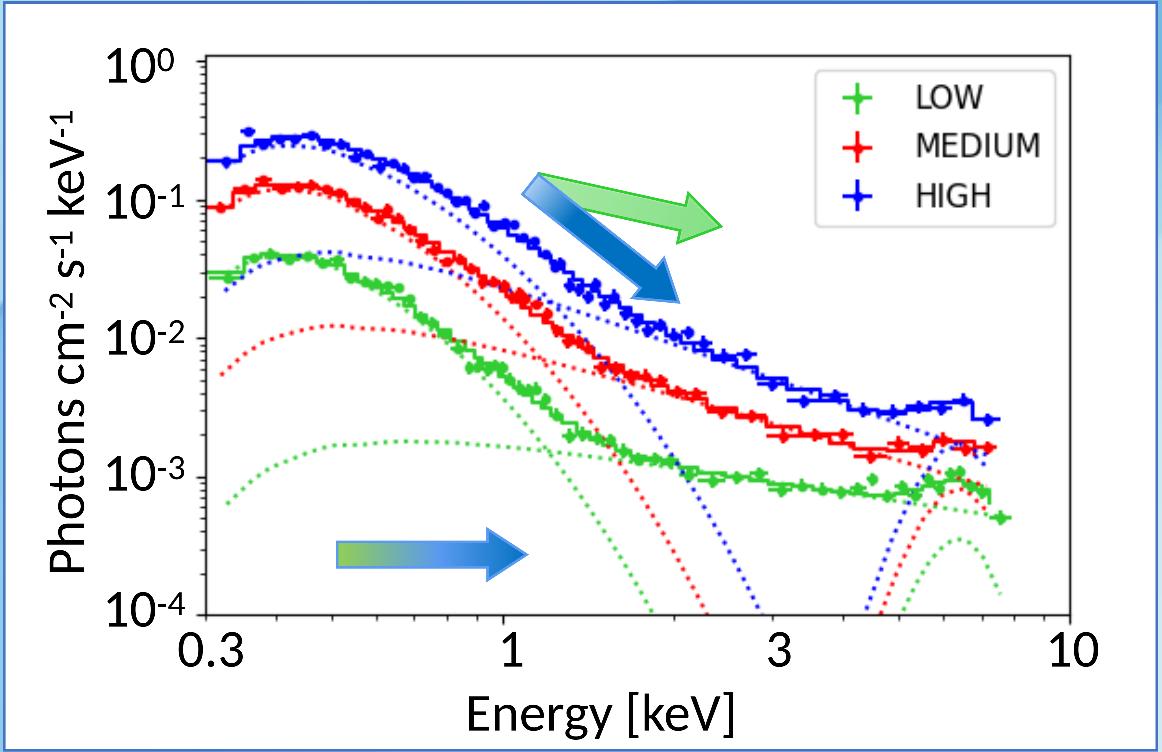

Luminosities 0.3—10 keV:

$1.33 \pm 0.02 \times 10^{38}$ erg/s

$6.13 \pm 0.02 \times 10^{37}$ erg/s

$2.45 \pm 0.05 \times 10^{37}$ erg/s

- Composite Spectrum:
  - soft thermal component (kT~0.2 keV, ~30—40% F_{TOT})
  - hard non-thermal component (Γ~1.2)
  - broad emission line E=6.4 keV, σ~1 keV
- Spectral shape variations as a function of CR:
  - kT increases as CR increases
  - Γ steepens as CR increases

MR+ in prep.

Spectral Analysis — Infra-Bursts

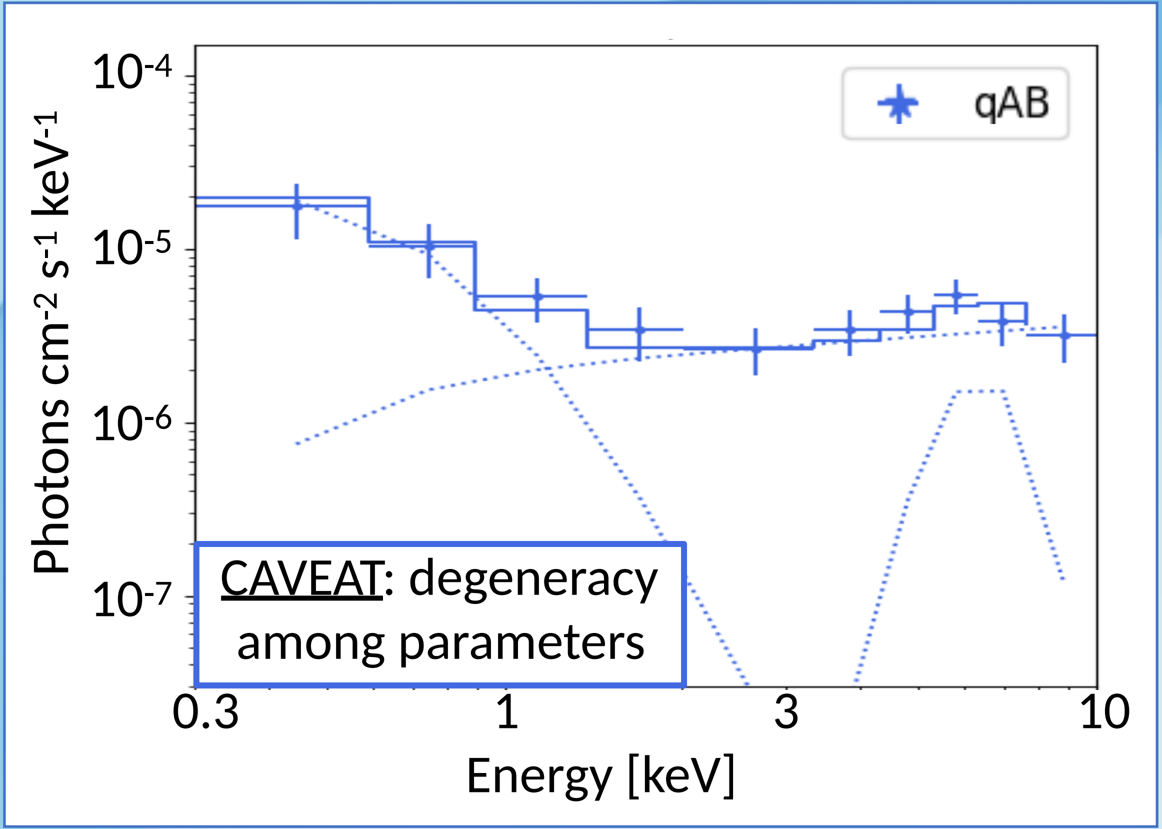

Luminosity 0.3—10 keV:

$(9 \pm 1) \times 10^{34}$ erg/s

- ✴ Composite Spectrum:
  - soft thermal component (kT~0.1—0.5 keV, ~5% F_{TOT})
  - hard non-thermal component (Γ~0)
  - broad emission line E=6.4 keV, σ~1 keV
- ✴ Spectral shape variations follow the behaviour of Burst spectra, and the thermal component changed the most

MR+ in prep.

Spectral Analysis — Quiescence

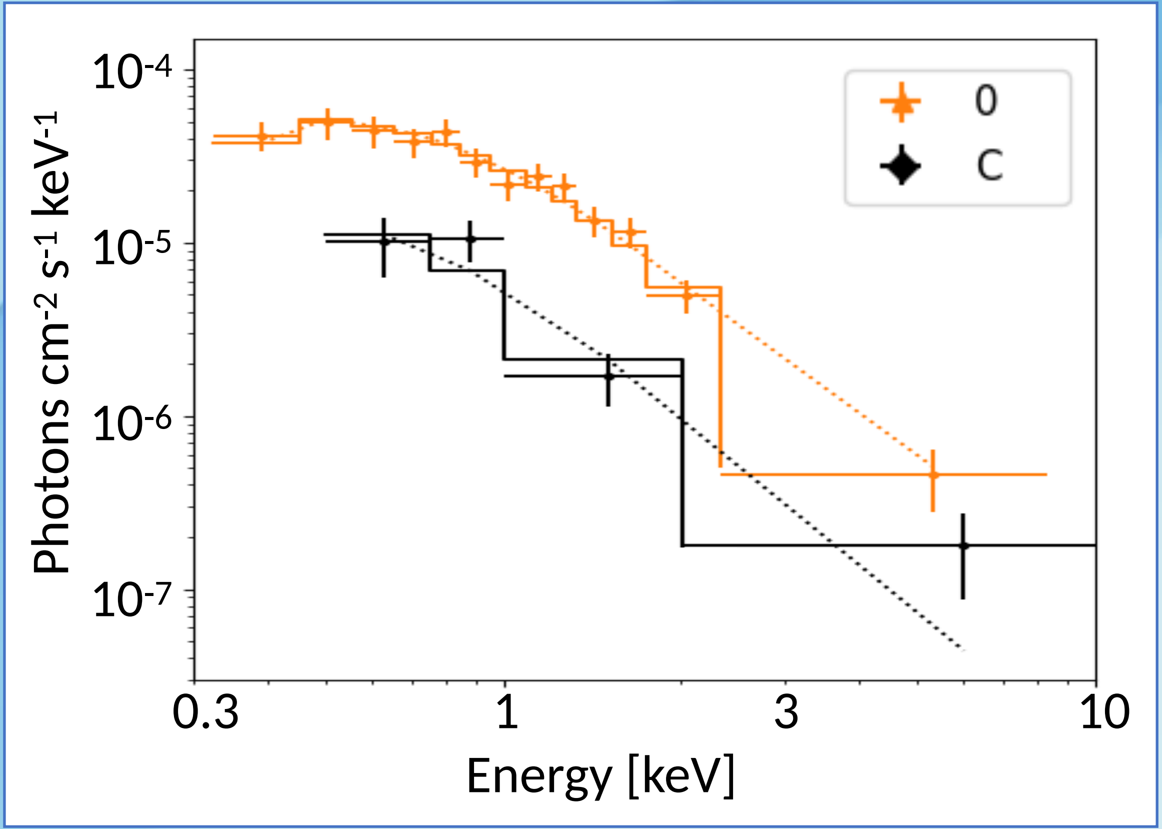

Luminosities 0.3—10 keV:

$(3.3 \pm 0.2) \times 10^{34}$ erg/s

$(6 \pm 2) \times 10^{33}$ erg/s

- Quiescence 2002 (0): soft emission
  - Bremsstrahlung —> kT~1.0 keV
  - BB —> kT~0.2 keV, R~3 km
  - PL —> Γ~3
- Quiescence 2018 (C): soft emission
  - Bremsstrahlung —> kT~1.4 keV
  - BB —> kT~0.3 keV, R~4 km
  - PL —> Γ~3

MR+ in prep.

Discussion

- Bursting activity never observed before in BeXBs in terms of:
  - Duration of the bursts (tens of seconds wrt hours/days)
  - Intensity of the 'soft excess' for large R_{BB}~300 km (~30—40% wrt 5% of F_{TOT})

data from
Fortin+ 2023, A&A
Townsend+ 2011, MNRAS

Discussion

- Bursting activity never observed before in BeXBs in terms of:
  - Duration of the bursts (tens of seconds wrt hours/days)
  - Intensity of the 'soft excess' for large R_{BB}~300 km (~30—40% wrt 5% of F_{TOT})

$$R_{NS} = 10 \text{ km}$$
$$R_{co} = 280 \text{ km}$$
$$R_M = 440 \text{ km } \xi \, L_{38}^{-2/7} B_{11}^{4/7}$$

- Can be explained invoking:
  - Short P_{spin} = 69 ms —> Small R_{co} = 280 km ~ R_M —> magnetic gating

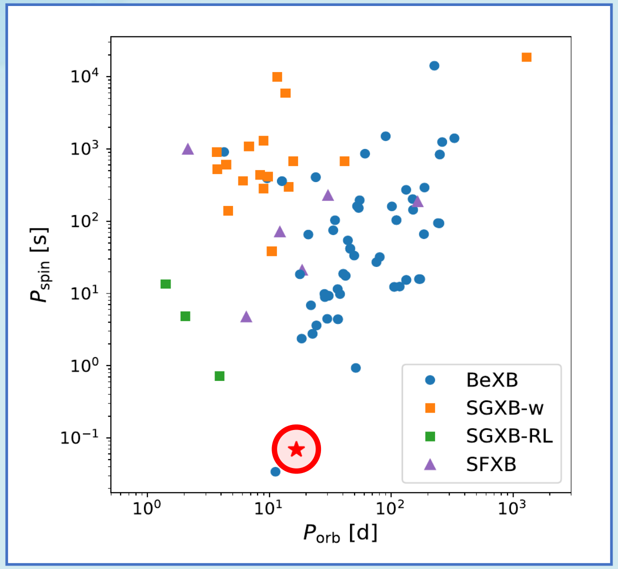

data from
Fortin+ 2023, A&A
Townsend+ 2011, MNRAS

Discussion

- Bursting activity never observed before in BeXBs in terms of:
  - Duration of the bursts (tens of seconds wrt hours/days)
  - Intensity of the 'soft excess' for large R_{BB}~300 km (~30—40% wrt 5% of F_{TOT})
- Can be explained invoking:
  - Short P_{spin} = 69 ms —> Small R_{co} = 280 km ~ R_M —> magnetic gating
  - Eccentric orbit (e=0.72) —> Close-by periastron passage —> strong and variable interaction with Be wind and disk (warped, tilted, not always present)

$$R_{NS} = 10 \text{ km}$$
$$R_{co} = 280 \text{ km}$$
$$R_M = 440 \text{ km } \xi \, L_{38}^{-2/7} B_{11}^{4/7}$$

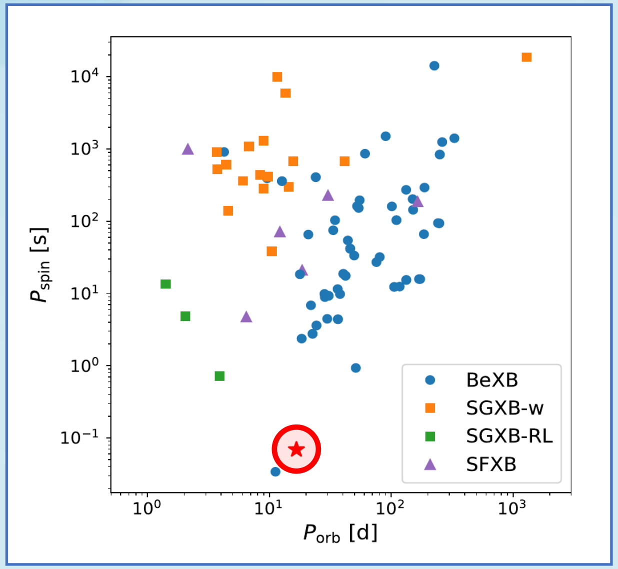

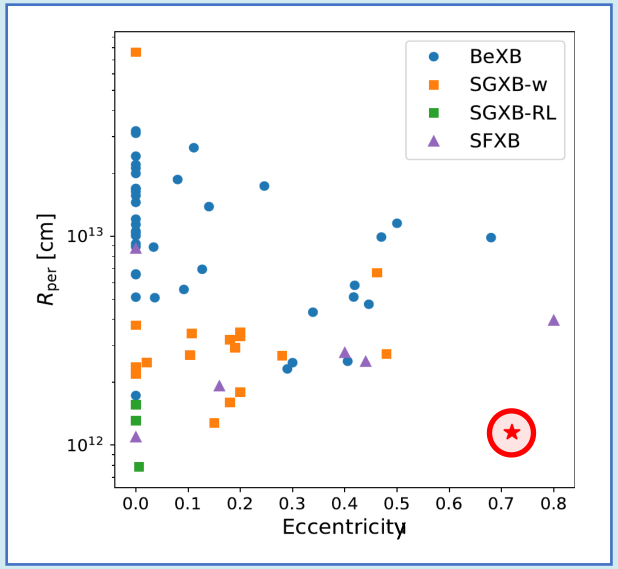

data from
Fortin+ 2023, A&A
Townsend+ 2011, MNRAS

Discussion

- Two possibilities to explain the spectra:
  - Hard is primary component (accretion column) and soft is reprocessing component
  - Soft is primary component (hot matter) and hard is Comptonized component

Discussion

- Two possibilities to explain the spectra:
  - Hard is primary component (accretion column) and soft is reprocessing component
  - Soft is primary component (hot matter) and hard is Comptonized component

$$R_{NS} = 10 \text{ km}$$
$$R_{co} = 280 \text{ km}$$
$$R_M = 440 \text{ km } \xi L_{38}^{-2/7} B_{11}^{4/7}$$

- Three emission regimes:
  - Bursts, $L_X \sim 10^{37}$—10^{38} erg/s —> Direct accretion regime —> $R_{NS} < R_M < R_{co}$ —> 10^8 G $< B < 10^{11}$ G
  - Infra-Bursts, $L_X \sim 10^{35}$ erg/s —> Weak propeller regime
  - Quiescence $L_X \sim 10^{33}$—10^{34} erg/s —> Strong propeller regime —> accretion is not possible, shocked material halted at R_M

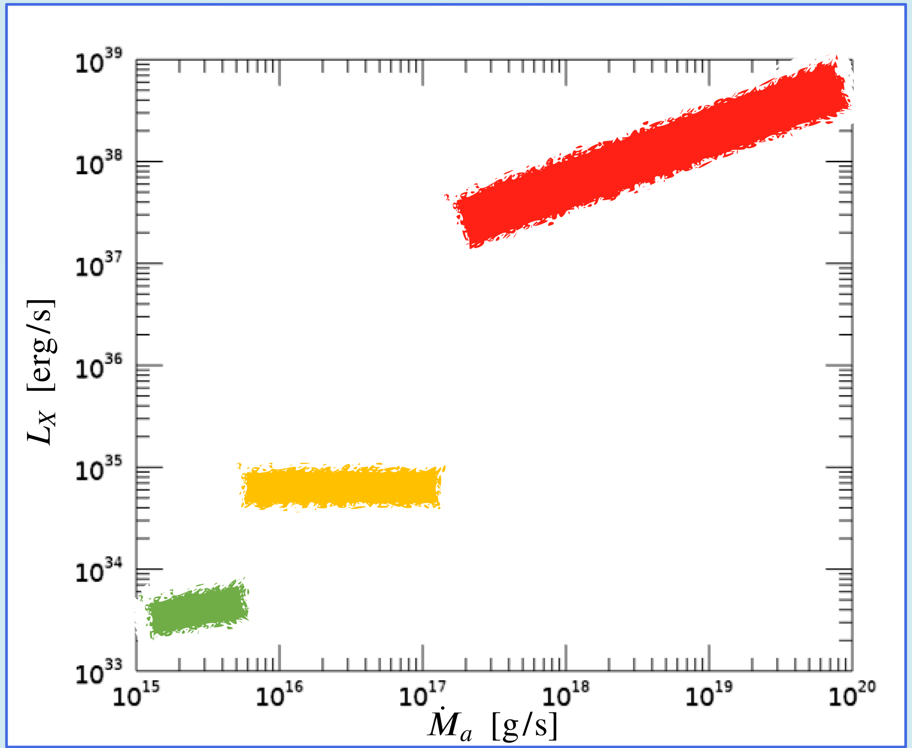

Summary and Conclusions

- Reanalysis of all the XMM-Newton observations of the BeXB A0538—66
  - Temporal characterization of the bursts
  - CR resolved spectra showed at least three different emission states

- Magnetic gating instabilities due to $R_M \sim R_{co}$, unusual in BeXBs because usually P_{spin} is larger
  - Explains the variability in obs A and B (hiccup direct accretion and weak propeller)
  - In C and 0 accretion is not possible, strong propeller, steady emission from shocked material at R_M

- Interpretation of the bulk emission is still open, no pulsations were detected (PF<15%)

- More similarities with other peculiar objects
  - AMSP IGR J18245—2452 (Ferrigno+ 2013), LMXB IGR J17407—2808 (Ducci+2023) [but different L_X]
  - Bursting Pulsar GRO 1744—28 (Court+ 2018) [but different ΔL]

Thanks for the attention!

Orbital Parameters

$P_{\rm spin}$	69 ms
$P_{\rm orb}$	16.64002 d
$P_{\rm sup}$	420.8 d
Dist	50 kpc
B	10^8 G $< B <$ 10^{11} G
M_*	$\leq 8.84\,\mathrm{M}_\odot$
$M_{\rm X}$	$1.44\,\mathrm{M}_\odot$
e	0.72
R_*	$\sim 10\ \ \mathrm{R}_\odot$
$i_{\rm orb}$	$\leq 75°$
$i_{\rm disc}$	$\gtrsim 70°$
a	4.15×10^{12} cm

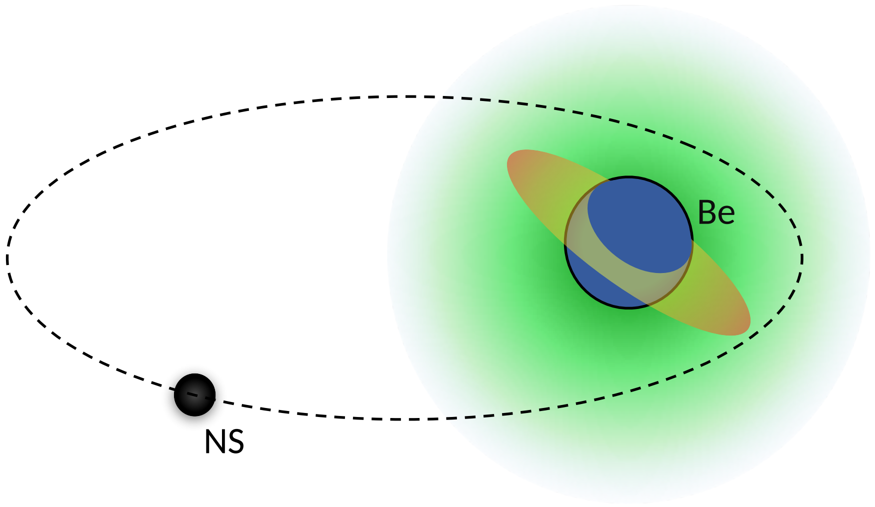

Two States

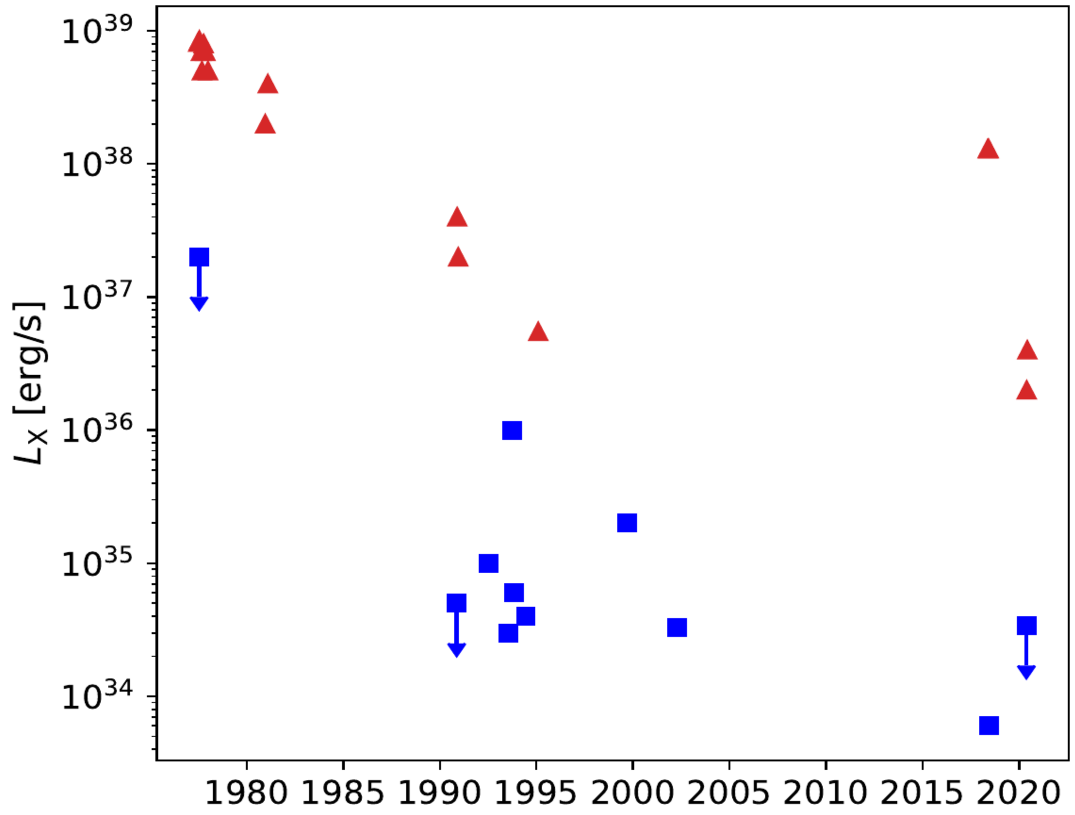

Flaring activity

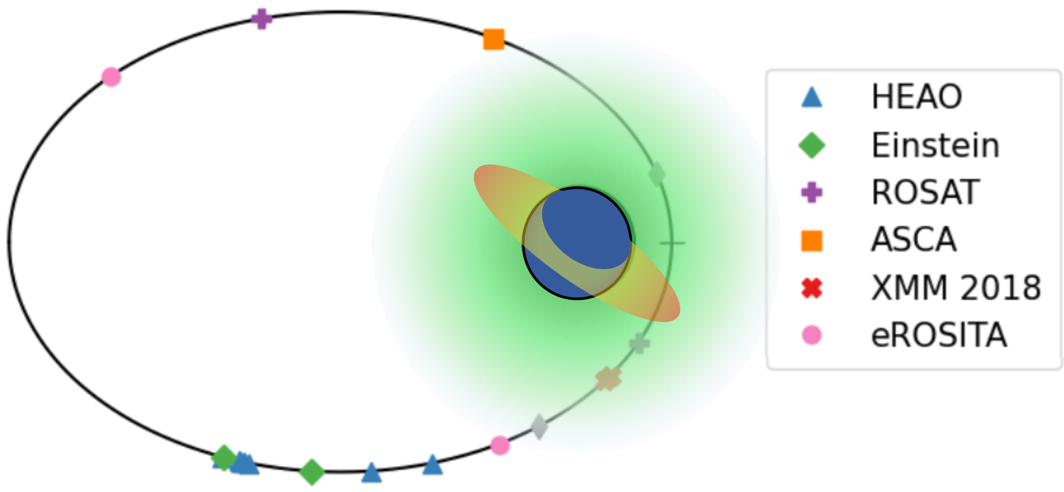

Quescient phase

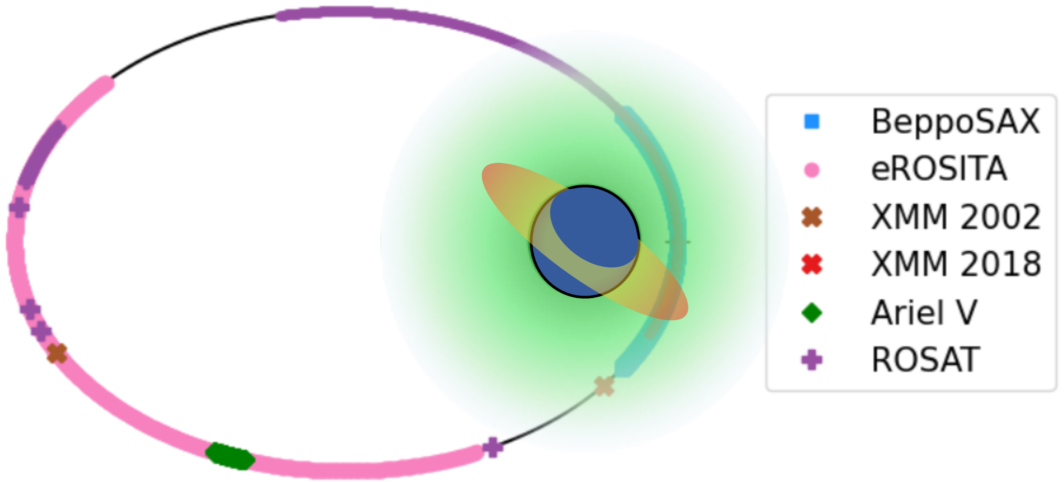

X-ray and optical flares

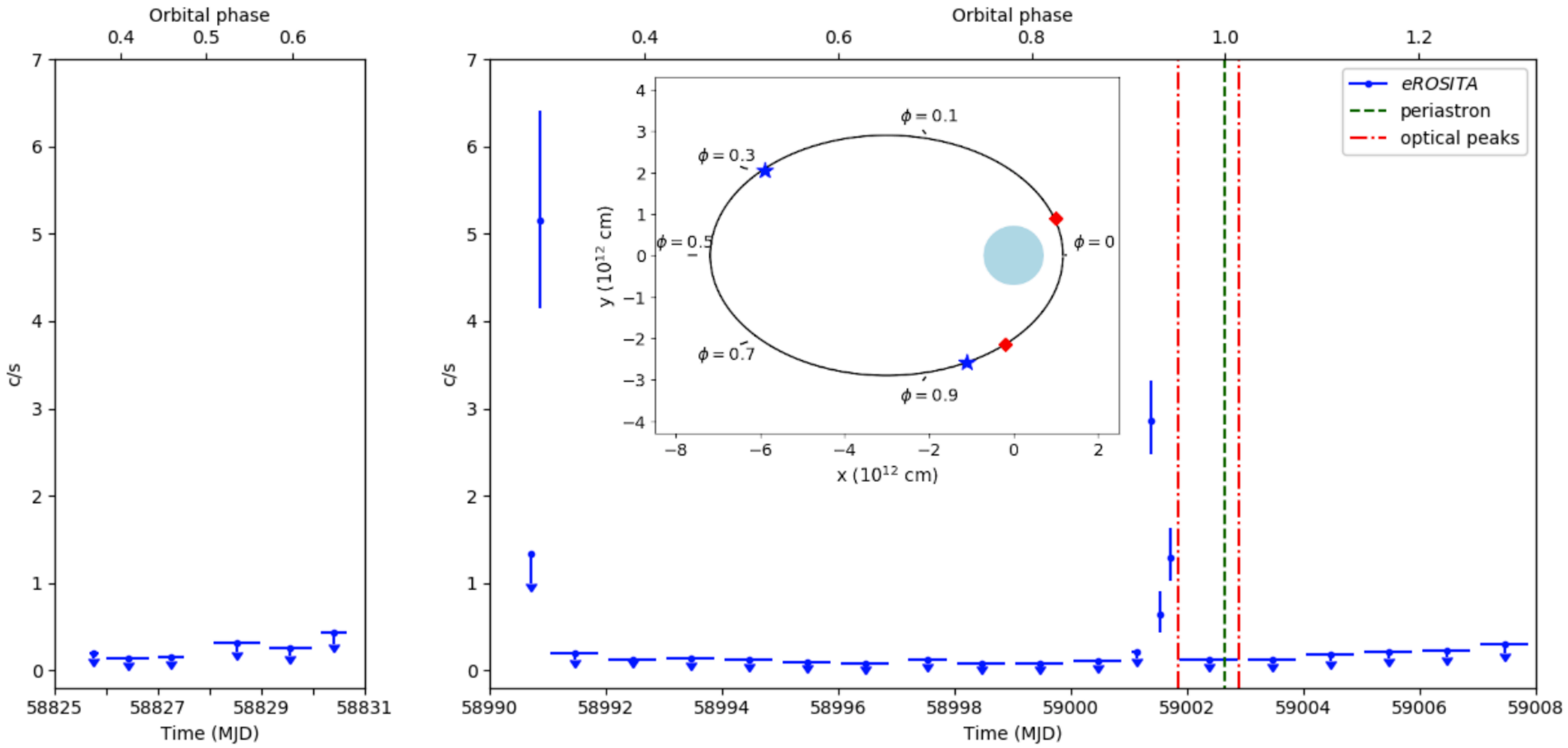

Fig. 4. eROSITA light curve (0.2–10 keV) of A0538−66 of the first sky survey. Each point during the flares represents one scan. Outside of the flares, the 90% c.l. upper limit was obtained by binning the data within one day. The top horizontal axis shows the orbital phase, and phase zero corresponds to the periastron passage. The inset shows the position of the eROSITA flares (blue stars) and of the optical peaks (red squares) in the orbit.

Burst statistics

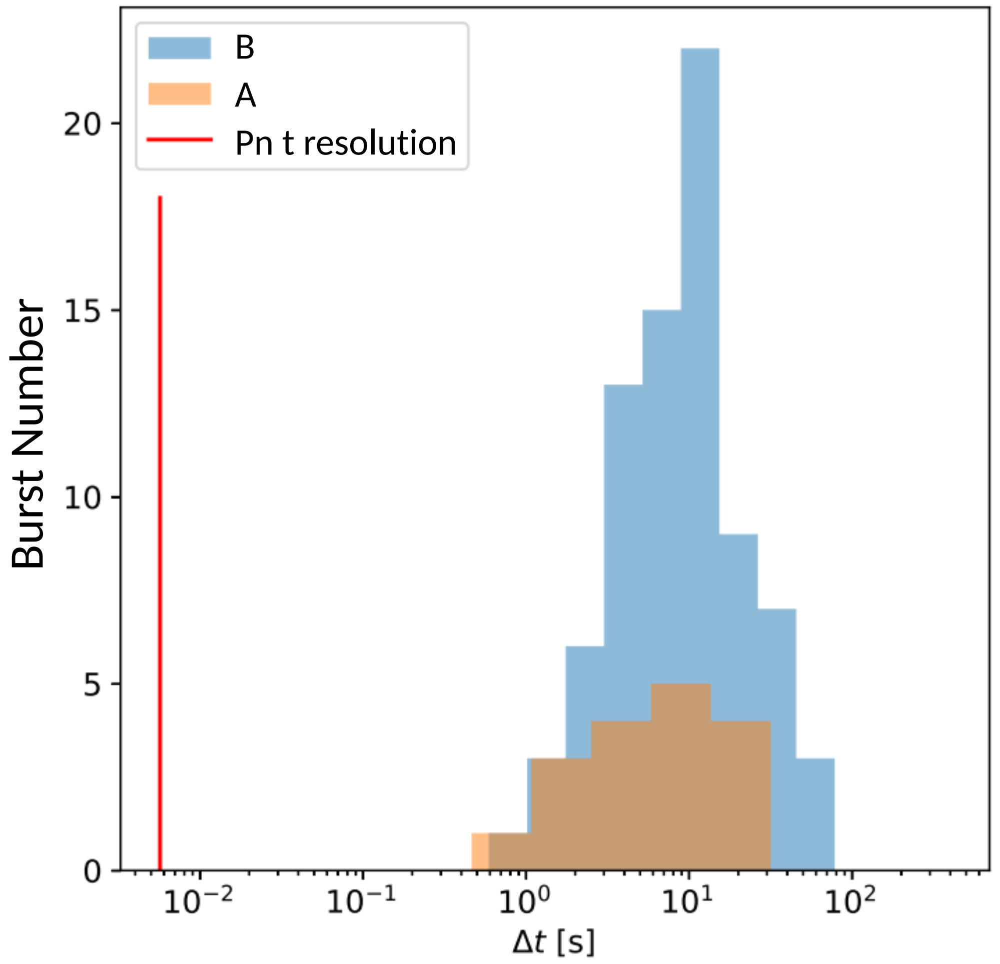

HR dependence

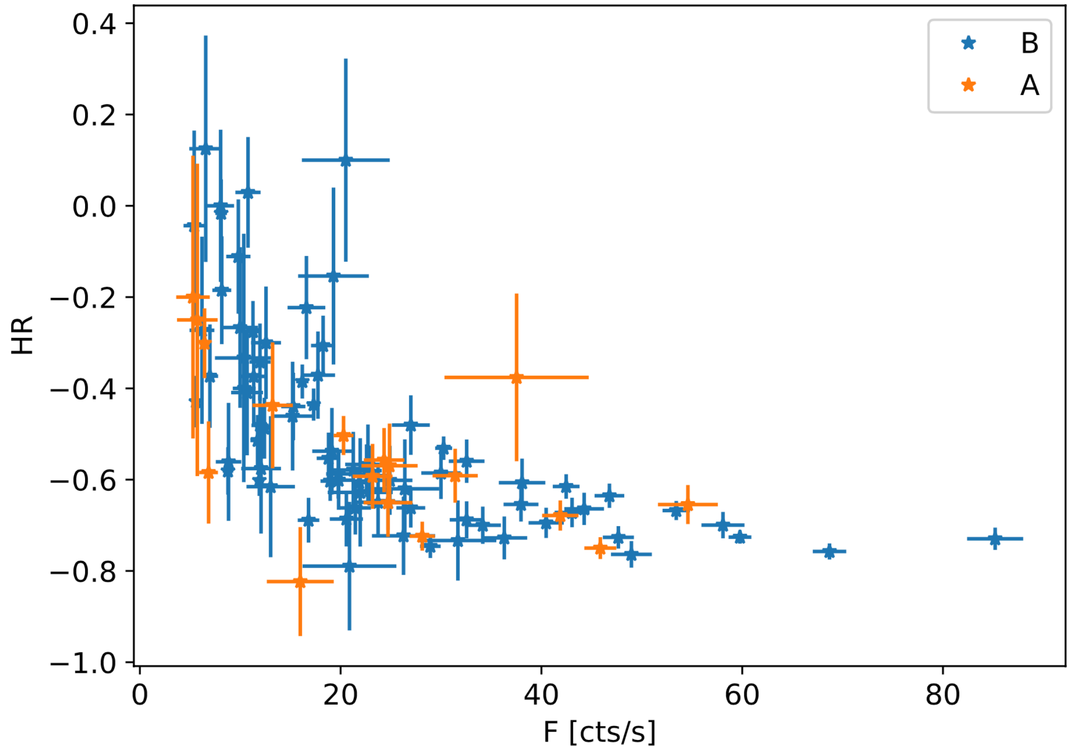

$$HR_i = \frac{C_{i+1} - C_i}{C_{i+1} + C_i}$$

Soft Band: $0.3 - 2$ keV

Hard Band: $2 - 10$ keV

HR dependence

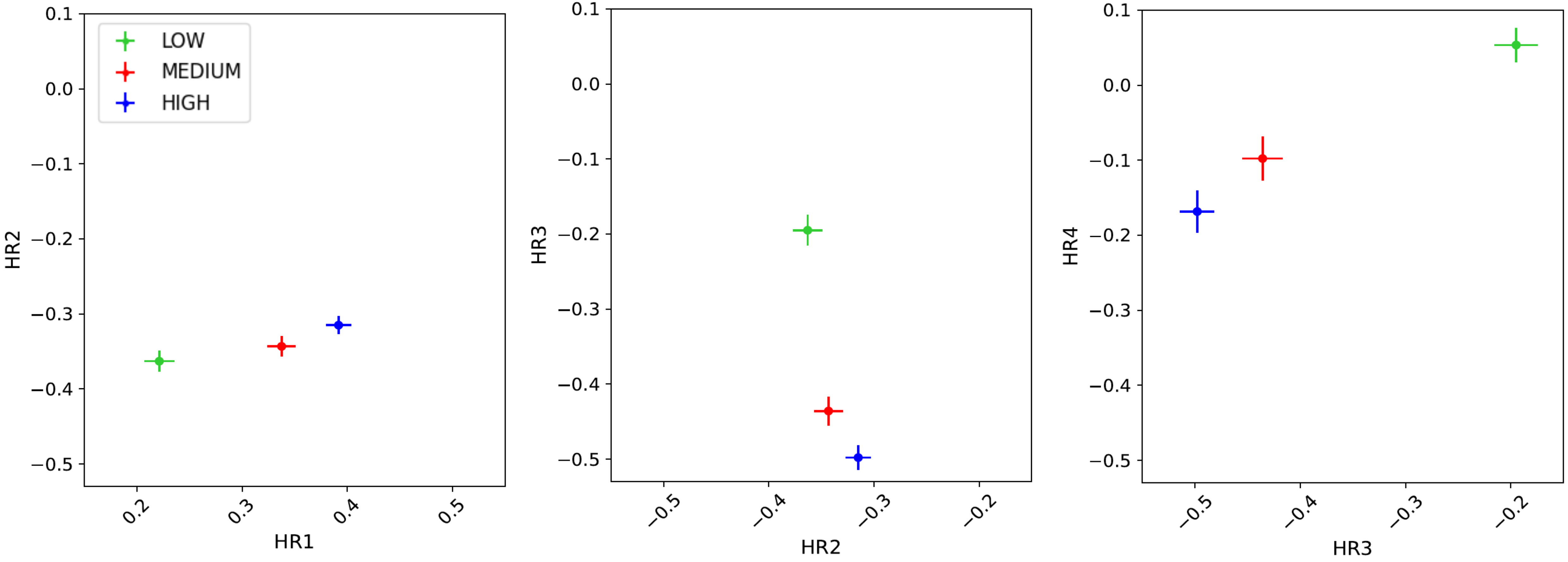

$$HR_i = \frac{C_{i+1} - C_i}{C_{i+1} + C_i}$$

Band 1: $0.3 - 0.5$ keV

Band 2: $0.5 - 1$ keV

Band 3: $1 - 2$ keV

Band 4: $2 - 4.5$ keV

Band 5: $4.5 - 10$ keV

Spectral Analysis — CR resolved Bursts

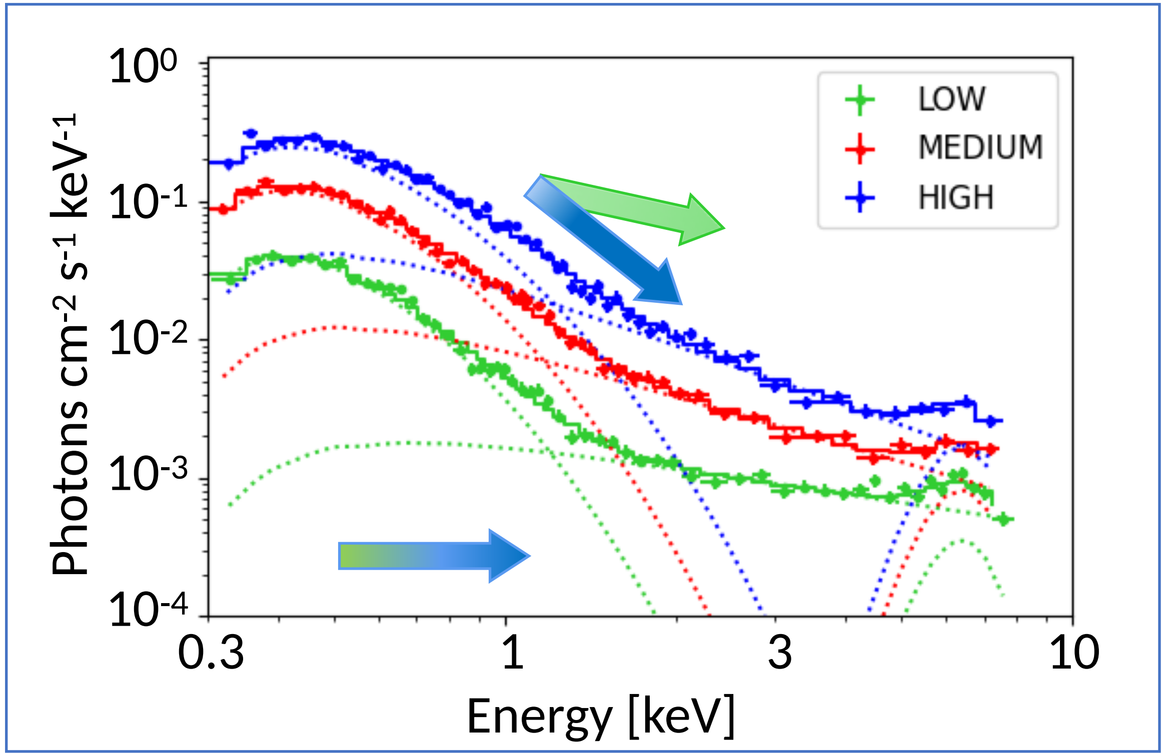

- Best fitting model - thermal component:
  - Bremsstrahlung —> kT = 0.30, 0.33 and 0.42 keV
  - DiskBB —> $R_{in}\sqrt{\cos i}$ = 240, 367 and 365 km
  - BB —> R = 420, 630 and 640 km
- Best fitting model - non-thermal component:
  - PL —> Γ = 0.6, 1.2, 1.4
  - Comptonization —> Γ = 1.1, 1.8, 1.9, kT_e=50 keV
- Best fitting model - iron line:
  - Gaussian emission line E = 6.4, σ = 1 keV
  - Diskline poorly costrained

Comparison with other binaries

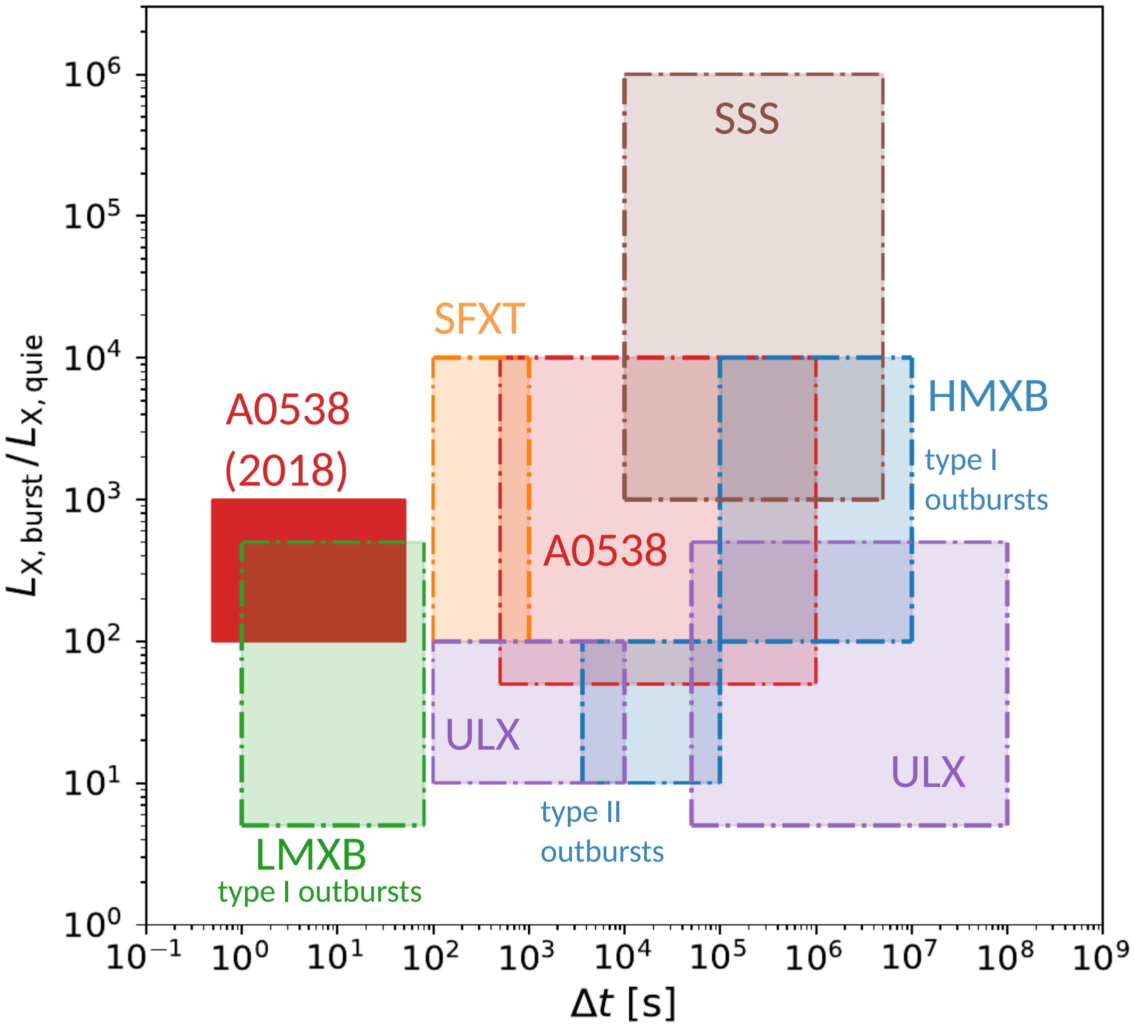

Comparison with other binaries

- BeXB
  - SAX J0635.2+0533: P=33.8 ms, P_{dot}<3.8x10^{-13} s/s —> E_{dot}<5x10^{38} erg/s; **L_{peak}~5x10^{32} $d^2_{5\ kpc}$ erg/s**, ΔL~10, Δt~days [La Palombara & Mereghetti 2017]
  - AX J0049.4—7323: **L_{peak}~10^{37} erg/s**, ΔL~270, Δt~days [Ducci+ 2018]
  - RX J0058.2—7231 and RX J0520.5—6932: very eccentric orbit and variable Be disk [Schmidtke+ 2003]
- LMXB
  - IGR J17407—2808: **L_{peak}~5x10^{36} $d^2_{2\ kpc}$ erg/s**, ΔL~1000, Δt~1—100 s [Ducci+2023]
  - 'Bursting Pulsar' GRO 1744—28 and 'Rapid Buster' MXB 1730—335: **L_{peak}~10^{37}—10^{38} erg/s**, ΔL~10—40, Δt~10 s [Bagnoli+ 2015, Court+ 2018]
- AMSP
  - IGR J18245—2452: P=3.9 ms, **L_{peak}~10^{36} erg/s**, ΔL~10, Δt~seconds; harder spectrum during the lower flux state [Ferrigno+ 2013]

X-ray Reprocessing

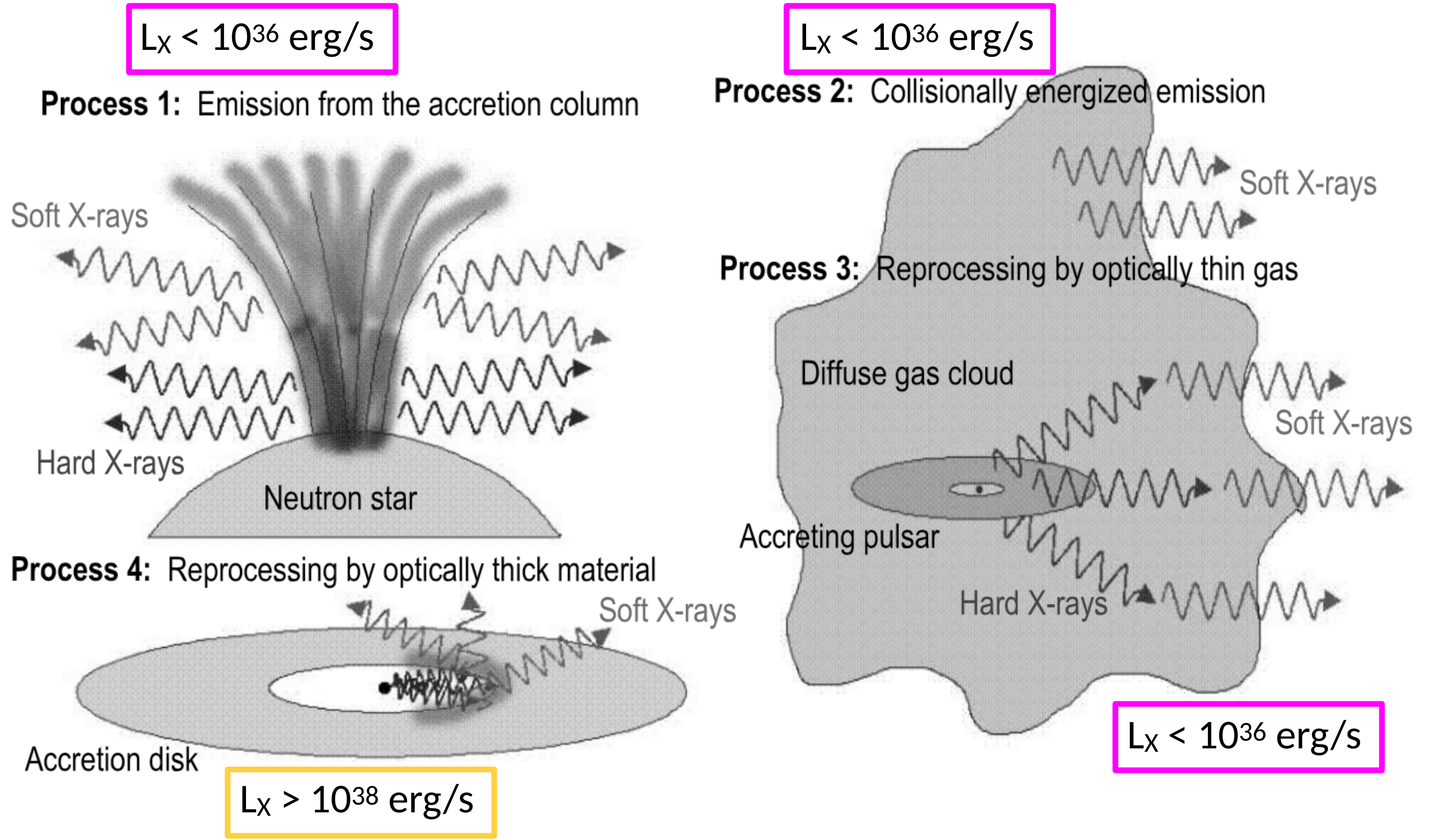

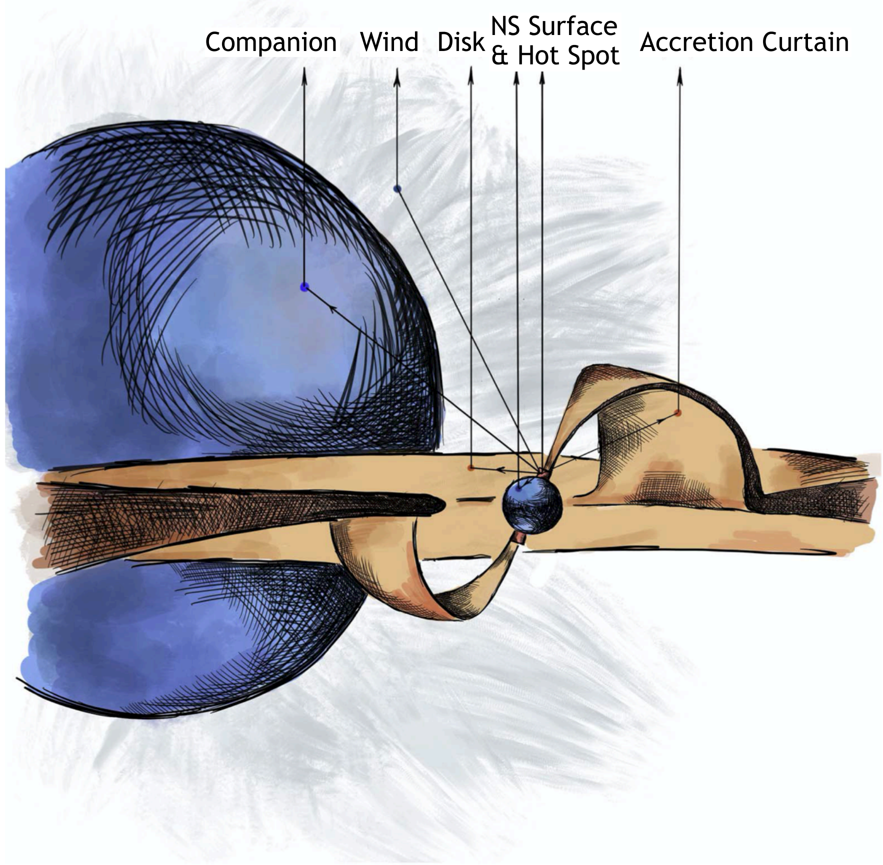

Hickox+ 2004, ApJ

Tsygankov+ 2022 ApJ

Characteristic Radii

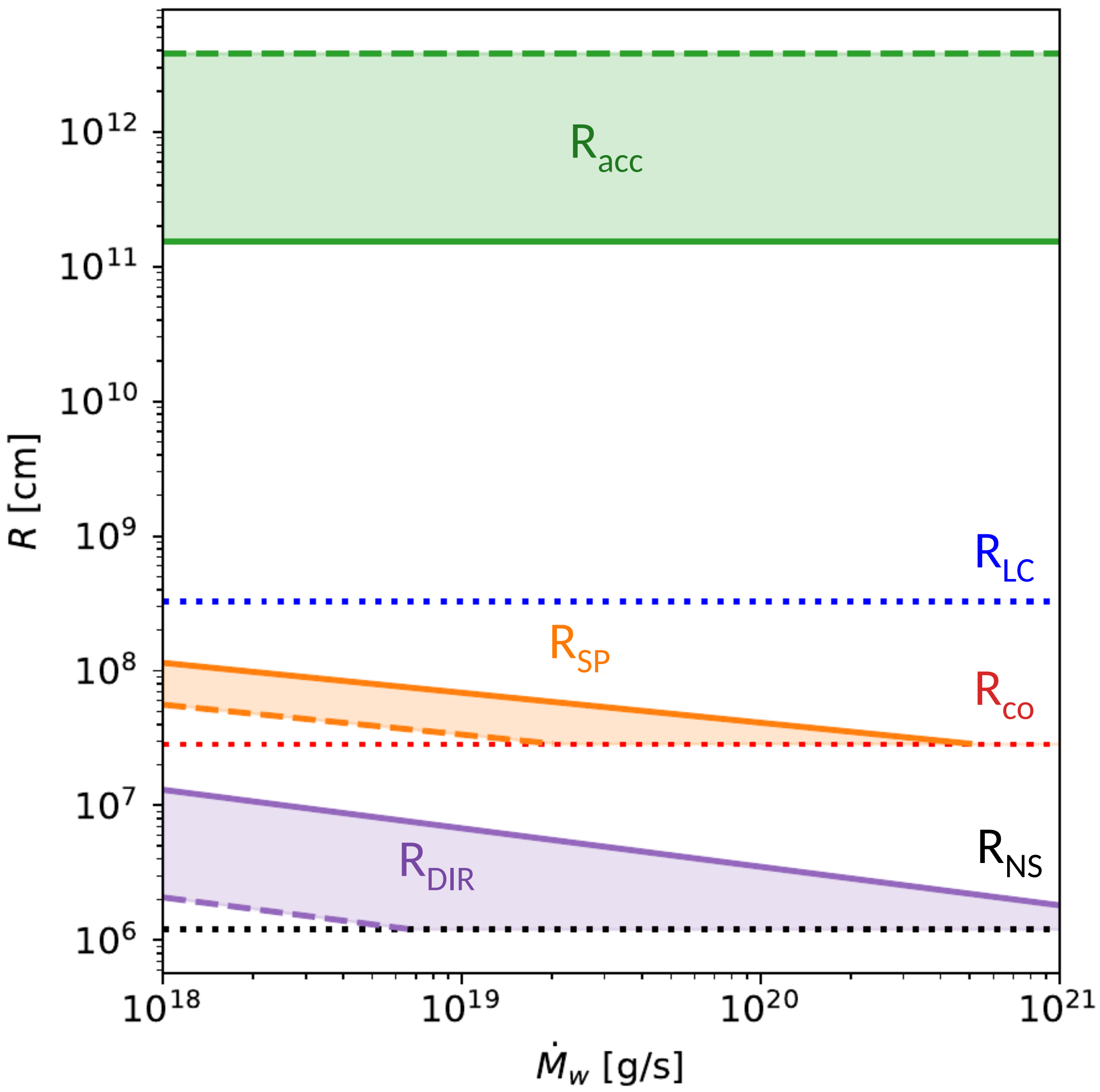

$$R_{\rm acc} = \frac{2\,GM_{\rm NS}}{v_w^2}$$

$$R_{\rm LC} = \frac{cP_{\rm spin}}{2\pi}$$

$$R_{\rm co} = \left(\frac{G\,M_{\rm NS}\,P_{\rm spin}^2}{4\pi}\right)^{1/3}$$

$$R_{\rm SP} = \left(\left(\frac{32}{3}\right)^{3/2}\frac{1}{2}\right)^{-2/9} G^{-1/3} M_{\rm X}^{-1/3} \dot{M}_{\rm w}^{-2/9} v_{\rm rel}^{4/9} a^{4/9} \mu^{4/9}$$

$$R_{\rm DIR} = \left(\left(\frac{32}{5}\right)^{5/2}\frac{1}{2}\right)^{-2/7} G^{-5/7} M_{\rm X}^{-5/7} \dot{M}_{\rm w}^{-2/7} v_{\rm rel}^{8/7} a^{4/7} \mu^{4/7}$$

Accreting regimes

Direct Accretion

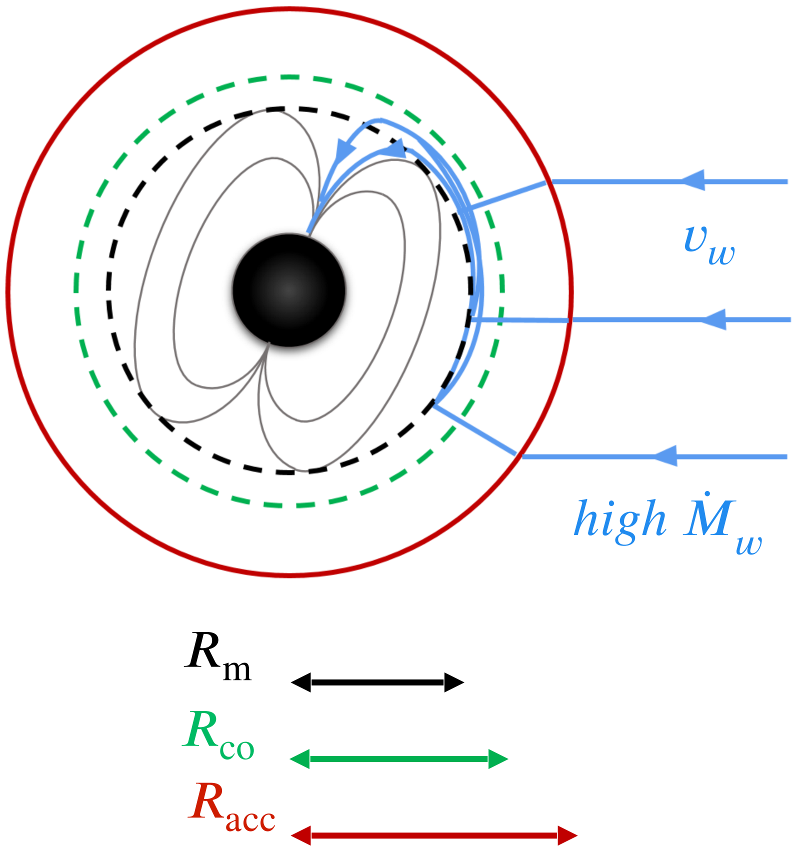

Weak Propeller

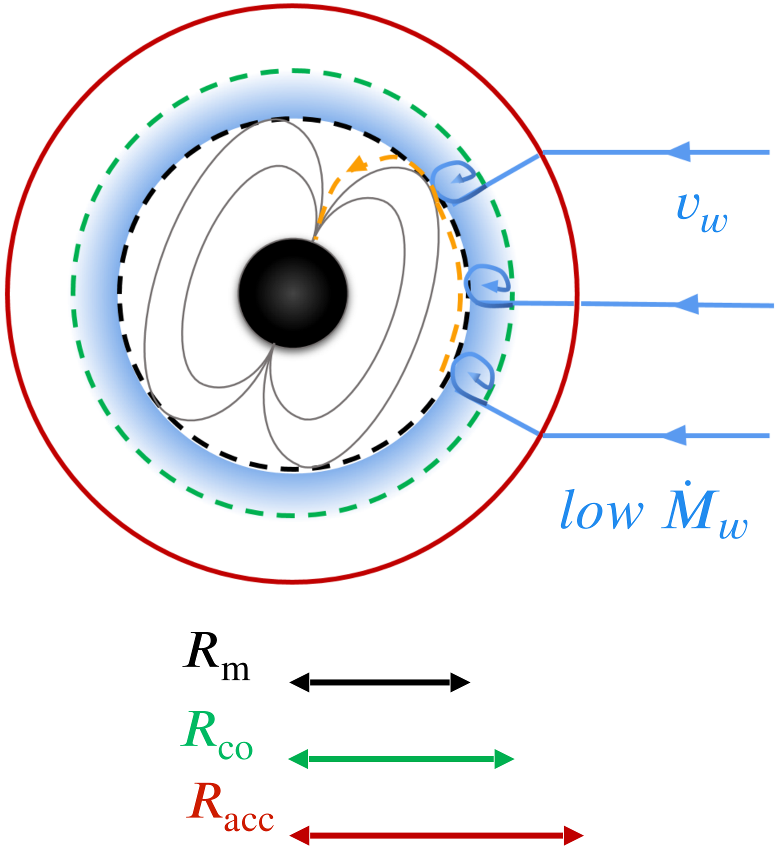

Strong Propeller

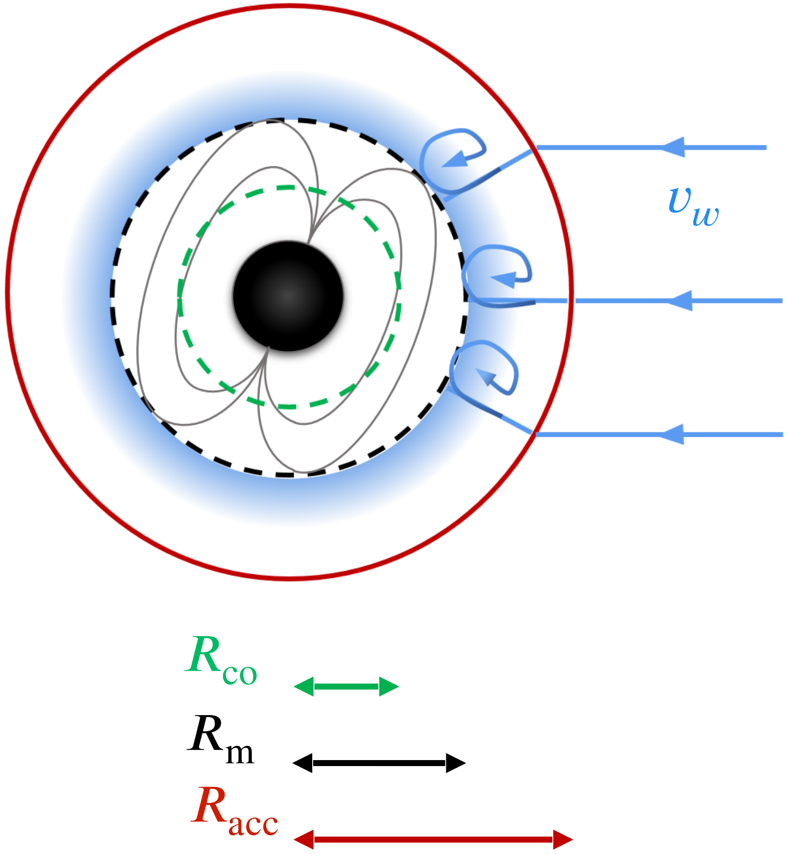

$$\dot{M}_{lim} = 2.8 \times 10^{-4} \left(\frac{P_{\rm spin}}{10^3\ {\rm s}}\right)^{-3} \left(a_{\rm 10d}(1-e)\right)^2 \left(\frac{v_w}{10^8\ {\rm cm/s}}\right) \left(\frac{R_{\rm m}}{10^{10}{\rm cm}}\right)^{5/2} \left[1 + \frac{16 R_{\rm acc}}{5\ R_{\rm m}}\right] {\rm M}_\odot/{\rm yr}$$

Wind accretion luminosities